JOURNAL OF THERMOPHYSICS AND HEAT TRANSFER
Vol. 16, No. 1, January–March 2002

Growth Rate of Crystallization in Disodium Hydrogenphosphate Dodecahydrate

Satoshi Hirano*
National Institute of Advanced Industrial Science and Technology, Tsukuba 305-8569, Japan
and
Takeo S. Saitoh†
Tohoku University, Sendai 980-8579, Japan

The solidification process of disodium hydrogenphosphate dodecahydrate was investigated to develop long-term latent heat storage that uses supercooling. Supercooled thermal energy storage (Super-TES) stores thermal energy at temperatures lower than the melting point of the phase-change material (PCM), thus reducing the heat loss from the storage system. During nucleation and solidification, the temperature of PCM is not constant in Super-TES. The solidification process in Super-TES, therefore, influences the performance of the storage system because thermal properties of PCM, strongly depend on the temperature and phase of the material. The results show that the growth rate of the hydrate increased with increasing degree of supercooling and that this growth rate was slow compared with that of metals. When the degree of supercooling was less than about 10 K, the crystal of the hydrate grew like a single crystal, and the growth rate was approximately proportional to the third power of the degree of supercooling. Because the viscosity of the hydrate in the liquid phase below the melting point increased drastically, when the degree of supercooling exceeded about 10 K, the crystal grew like a dendritic crystal, and the increase in the growth rate with increasing degree of supercooling decreased.

Nomenclature

a	=	lattice constant, m
h	=	Planck's constant, J · s/molecule
I	=	nucleation rate, 1/s · m^3
k	=	Boltzmann's constant, J/K · molecule
N	=	Avogadro's number, molecules/mol
n	=	number of molecules
r^*	=	critical radius for homogeneous nucleation, m
T_e	=	equilibrium temperature, K
T_n	=	nucleation temperature, K
V_M	=	molar volume, m^3/mol
v	=	growth rate, m/s
ΔF_a	=	free energy of activation for transporting a molecule across the liquid–crystal interface, J/molecule
ΔH	=	heat of fusion, J/kg
ΔT	=	degree of supercooling, defined as $T_e - T_n$, K
δ	=	thermal diffusion range, m
η	=	viscosity, Pa · s
λ	=	thermal conductivity, W/m · K
ρ	=	density, kg/m^3
σ_{SL}	=	interfacial free energy, J/m^2

Subscripts

l	=	liquid conditions
s	=	solid conditions

Received 18 December 2000; revision received 7 May 2001; accepted for publication 2 August 2001.

*Senior Research Scientist, Institute for Energy Utilization, 16-1 Onogawa.

†Professor, School of Aeronautics and Space Engineering, 01 Aramaki-Aoba.

Introduction

GLOBAL warming and depletion of fossil fuels are two problems that are caused by large-scale energy consumption. To resolve these problems, the current practice of focusing on inexpensive energy use should be abandoned, and the focus should be shifted to efficient energy use that does not adversely affect the environment. Thermal energy storage is important for the efficient generation and use of energy because it can store energy during slack demand times, for example, at night, and provide energy during high demand times, for example, during the day. To meet a given peak demand, energy storage permits smaller power plants to be built, and it also permits them to be run continually at peak operating efficiency. Such energy storage devices are also important for smoothing out power-generation cycles for solar and wind power generation, where power can only be produced during daylight (solar power) or under windy conditions (wind power).

Two types of thermal energy storage are now in use: sensible heat thermal energy storage (SHTES) and latent heat thermal energy storage (LHTES). LHTES uses a phase-change material (PCM) and is desirable because compared with SHTES, LHTES systems transfer energy at constant temperature during a phase change, thus permitting high-energy-storage density and stable output temperature. Therefore, for applications where the space used by energy storage systems must be minimized, LHTES is more suitable than SHTES. Whereas most LHTES systems are developed for short-term storage, in this work we considered the possibility of using the supercooling behavior of PCMs to develop long-term LHTES systems.

Figure 1 shows typical temporal temperature variation for the solidification of one type of PCM, disodium hydrogenphosphate dodecahydrate (DHD), $Na_2HPO_4 \cdot 12H_2O$, where this hydrate is cooled from the liquid phase at a constant rate of 0.3°C/min in a test tube submersed in a water bath. Although the melting point of the hydrate is about 36°C, crystallization does not start until the liquid is supercooled to 23°C. After crystallization starts, the temperature of the hydrate increases to its melting point, and the hydrate releases energy equal to its heat of fusion until solidification is completed.

Supercooled thermal energy storage (Super-TES) uses this temperature hysteresis between fusion and solidification to store energy. A typical operating mode of Super-TES is as follows. The PCM is

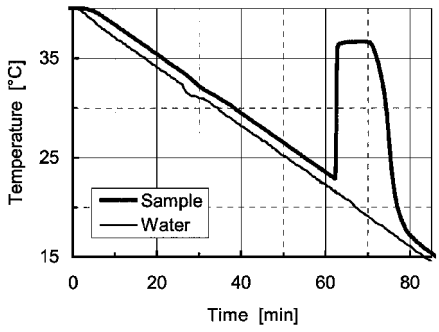

Fig. 1 Temporal temperature variation of DHD during constant-rate cooling.

completely melted by using surplus heat in the summer and is left at room temperature without thermal insulation until winter. In the winter, the supercooled PCM is crystallized on demand, and the heat of fusion released from the PCM at a temperature higher than room temperature is used as an energy source. Therefore, compared with conventional storage systems, Super-TES systems can reduce heat loss from the storage system because energy is stored at a temperature close to room temperature.

During nucleation and solidification, the temperature of PCM is constant in a conventional latent heat storage system, but not in Super-TES. This means that the behavior of PCM during solidification in Super-TES influences the performance of the storage system because thermal properties of PCM, especially specific heat and thermal conductivity, significantly depend on the temperature and phase of the material. Except for water and metals, however, there is insufficient information in the open literature on the solidification process of materials used in heat storage devices. The current study evaluated the growth rate of crystallization and the critical radius for nucleation in DHD as a function of degree of supercooling, ΔT, which is defined as the difference between the equilibrium temperature T_e and the nucleation temperature T_n, that is, $\Delta T = T_e - T_n$. The results showed that the growth rate of the DHD increased with increasing ΔT and that this growth rate was slow compared with that of metals. The estimated interfacial free energy was on the order of 10^{-2} J/m^2.

Materials and Methods

DHD Sample

DHD is a promising PCM for Super-TES because it is less toxic and cheaper than most other hydrates. The probability that nucleus formation is initiated in the supercooled hydrate by physical vibration and the possibility that disodium hydrogenphosphate segregates from the hydrate are also lower than for most other hydrates. The melting point of DHD also makes this hydrate suitable for space heating. The sample used in this study conformed to the specifications for special reagent-grade DHD of the Japanese Industrial Standard (JIS) K9019-1996. The chemical content of DHD is listed in Table 1. The DHD is efflorescent. In room air, the crystal water of the hydrate gradually evaporates, and dodecahydrate changes into heptahydrate or dihydrate. Therefore, the measurement was done for DHD in a sealed test tube. One side effect of using a sealed tube is a change in pressure caused by thermal expansion. The effect on phase equilibrium, however, is negligible because change in pressure was estimated to be less than 1% for the temperature range studied here.

Melting point and heat of fusion are the most important thermophysical properties of PCMs. In this study, these two properties were measured by using a differential scanning calorimeter (DSC). The measured melting point was 35.54°C. The probable error of the measurement was ±0.38°C, which is the sum of the calibration error of the platinum resistance thermometer of DSC of ±0.1°C and the precision error of each measurement, ±0.28°C. The quoted error in this paper is this maximum error limit, which consists of calibration error and precision error. The measured heat of fusion was 265.6 kJ/kg, and the measurement error was ±3.7 kJ/kg. The purity of the hydrate used in this study was estimated to be 99.66% (+0.28/−0.43%) by fitting a portion of the DSC data to the Van't Hoff relationship (see Ref. 1). The density in the solid phase and in the liquid phase at the melting point was 1.52×10^3 and 1.45×10^3 kg/m^3, respectively. The probable measurement error of the density was ±6 kg/m^3. The specific heat in the solid phase and in the liquid phase at 25°C was 1.96 ± 0.02 and 3.43 ± 0.04 kJ/kg · K, respectively.[2]

Table 1 Chemical composition of a sample of disodium hydrogenphosphate dodecahydrate (JIS K9019-1996)

Description	Value
Purity	Minimum 99.0%
pH (50 g/l, 25°C)	9.0–9.4
Chloride	Maximum 0.001%
Sulfate	Maximum 0.005%
Heavy metals (as Pb)	Maximum 0.001%
Calcium	Maximum 0.02%
Arsenic	Maximum 1 ppm
Iron	Maximum 5 ppm
Ammonium	Maximum 0.001%

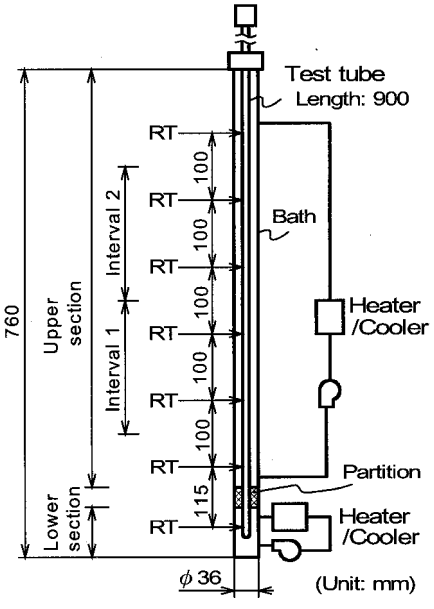

Fig. 2 Experimental apparatus for determining the growth rate of crystallization.

Experimental Procedure

The experimental apparatus used to measure the growth of crystallization in DHD is shown in Fig. 2. The sample was poured into two test tubes of different size made of heat-resistant glass to evaluate the influence of the surface tension of the DHD on the measurement of growth rate. One test tube had a 5.6-mm inner diameter and an 8-mm outer diameter, and the other had a 3.6-mm inner diameter and 6-mm outer diameter, and both were 900 mm long. Hereafter, these test tubes are called the 5.6-mm test tube and 3.6-mm test tube, respectively. The upper inlet of the test tube was sealed with a silicone stopper. The level of the sample was 630 mm from the bottom of the test tube. When the 5.6-mm test tube was quickly turned upside down, the air in the test tube slowly traveled up the tube, while the liquid DHD simultaneously traveled down the tube. When the 3.6-mm test tube was quickly turned down, however, the air and the hydrate in the test tube did not exchange their positions because of the surface tension of the hydrate. This means that the smaller test tube (3.6-mm test tube) can act as a capillary tube for the DHD.

The crystal growth was measured by placing each test tube in the axial center of a long cylindrical water bath (Fig. 2). The water bath

was partitioned into two sections by using thermal insulation; the lower section (90 mm high) was for initiating the crystallization, and the upper (600 mm high) was for observing the growth of crystals. The test tube resided in both sections. The temperature of each section was individually controlled. The vertical temperature distribution of the water circulating through the bath was measured by using platinum resistance thermometers (RT in Fig. 2). The probable error of each temperature measurement was within $+0.07/-0.11$°C.

The circulating water of the bath was cooled at a constant rate until the temperature reached a set value, and then kept constant at that temperature for more than half an hour to equilibrate the temperatures between the sample and the water. After the equilibration, only the lower section was cooled again to initiate crystallization. Because the sample is clear in the liquid phase, the crystals can be observed growing from the bottom of the test tube to the top. The growth rate of the crystal in the vertical direction was determined by measuring the time for the tip of the crystal to grow past each of two intervals (1 and 2) along the test tube, as shown in Fig. 2. The nominal distance for each interval was 200 mm, with the actual distance measured with a vernier caliper accurate to within ±0.03 mm. In the temperature range studied here, the change in length of the test tube caused by thermal expansion was negligible. The growth rates at the two intervals were measured using a stopwatch accurate to within ±0.0012% of the reading. The precision error for clocking the growth was estimated to be less than 0.7%. Consequently, the probable measurement error of the growth rate was within ±0.8%. After the measurement of growth rate, the sample in the test tube was reheated and completely melted to use next trial.

Results

Growth Rate

Figure 3 shows the measured growth rates of the crystal in the 5.6-mm test tube, showing that the growth rate is independent of the location in the vertical direction. The amount of the sample in the upper section of the 5.6-mm test tube was about 19 g. If the entire sample in the upper section solidifies at the same time, that is, simultaneously, the theoretical estimated temperature increase in the circulating water in the upper section is 0.03°C. In the experiment, the vertical distribution of the water temperature was within ±0.03°C, and the time fluctuation of the temperature was within ±0.06°C. The theoretical maximum temperature increase due to simultaneous solidification, 0.03°C, is less than the vertical temperature distribution and the temperature fluctuation of water with time. Therefore, the influence of the released heat of fusion into the circulating water on the observed growth rates was negligible in this experiment. The growth rate in the 3.6-mm test tube was also independent of the location along the test tube. Therefore, in the following sections, the growth rate plotted in Figs. 4, 6, and 8 is the average of the two growth rates for the two intervals.

Crystal Growth Process

Figure 4 shows the growth rates measured for the two test tubes as a function of ΔT. Although growth rate is related to interfacial free energy, there is no significant difference between the two results. The growth rate of the DHD sample was slow, ranging from 0 to 1 mm/s, compared with metals, whose growth rates range from 0 to 10^3 mm/s. The growth rate of DHD nonlinearly increased with ΔT. Several models have been proposed to explain the mechanism of crystallization of metals. For example, the following equations describe the growth rate based on the heat balance between the melt and crystal[3]:

$$v = \frac{2\lambda_l}{\Delta H \rho_s \delta}\Delta T \tag{1}$$

$$v = \frac{\lambda_l}{(\delta/r^*)\sigma_{SL}T_e}(\Delta T)^2 \tag{2}$$

Equation (1) shows that growth rate is proportional to thermal conductivity in the liquid phase, λ_l times ΔT. The thermal diffusion range δ is assumed to be the distance from the solid–liquid interface to the nearest point in the liquid where the temperature is considered identical to the liquid temperature located far from the interface. The estimated range of the thermal diffusion for the hydrate was 10^{-5}–10^{-4} m depending on ΔT. Equation (2) gives the maximum growth rate of Eq. (1) when the curvature of the growing surface is twice as large as the critical radius. Equation (2) shows that growth rate is proportional to thermal conductivity times the square of ΔT, that is, $(\Delta T)^2$.

The thermal conductivity of the DHD sample was measured by using the transient plane source technique described in detail elsewhere.[4–7] This technique allows the thermal conductivity of a small sample, about 50–100 g, from the solid phase to the liquid phase to be measured with the same sensor. Small samples are advantageous because they yield a larger ΔT for DHD, as mentioned later, resulting in wider temperature range for the measurement during supercooled conditions. The measurement error of the thermal conductivity was determined by using distilled water and clear quartz and found to be within ±3.0%. The sample temperature was measured with a calibrated copper–constantan thermocouple. The measurement error of the temperature was within ±0.2°C. Figure 5 shows the thermal conductivity of the sample as a function of degree of supercooling. For comparison, the thermal conductivity of water is also shown (solid line).[8] Figure 5 indicates that the thermal conductivity of DHD in the liquid phase, λ_l, is similar to the thermal conductivity of water and is relatively independent of ΔT for the temperature range studied here. Equations (1) and (2), therefore, show that the growth rate is either proportional to ΔT or to the square of ΔT, respectively. Growth rates of metals are generally proportional to ΔT when ΔT is low, <1 K. This relationship observed for metals was not observed for DHD in our experiments because the PCM is generally always cooled to supply heat, and ΔT is not low in the storage tank.

For most pure substances, especially metals, growth rates can be expressed by Eq. (2). For example, the growth rate of pure tin is proportional to the 1.8th power of ΔT (Ref. 9). Figure 6 shows the growth rate of the DHD sample as a function of ΔT on a log scale. For $4 < \Delta T < 10$ K, the growth rate follows a straight line and can be expressed as a least-squares approximation:

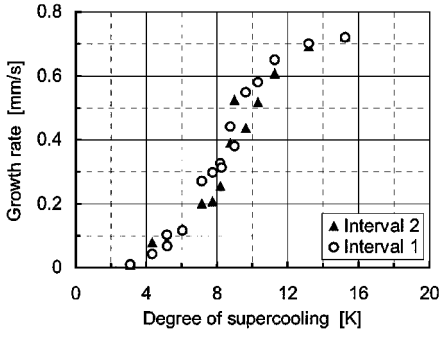

Fig. 3 Growth rate of the sample in the lower and the upper sections of a test tube with a 5.6-mm inner diameter.

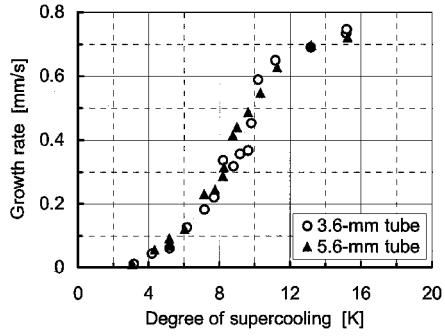

Fig. 4 Growth rate of the sample measured in two test tubes of different diameter.

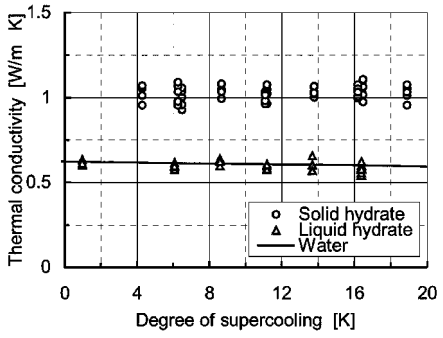

Fig. 5 Temperature dependence of thermal conductivity of DHD.

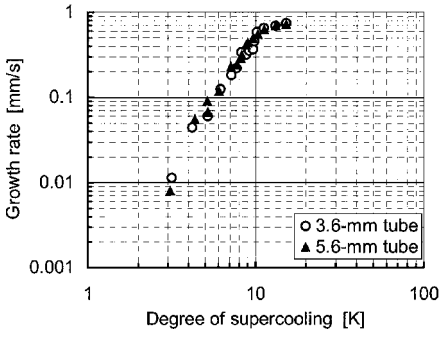

Fig. 6 Dependence of growth rate on degree of supercooling.

$$v = 7.15 \times 10^{-7}(\Delta T)^{2.85} \tag{3}$$

This approximation can not be used to express the measured growth rate for $\Delta T > 10$ K.

Another model to explain the mechanism of crystallization of metals has been proposed,[10] based on screw dislocation on a coarse surface as follows:

$$v = \frac{V_M \rho_s^2 (\Delta H)^2}{4\pi^2 a N \sigma_{SL} T_e^2} \cdot \frac{(\Delta T)^2}{\eta_l} \tag{4}$$

The molar volume and the heat of fusion of some finite weight of the sample is considered constant, and the density in the solid phase is considered constant in the temperature range studied here. The lattice constant of the sample and Avogadro's number are considered constant, and the equilibrium temperature is considered constant as long as pressure is constant. Then, Eq. (4) shows that the growth rate is proportional to the square of ΔT, but also shows that the growth rate is inversely proportional to the viscosity of the sample, η_l, times the interfacial free energy σ_{SL} between crystal nuclei and the corresponding liquid.

In our experiments, the viscosity of the sample was measured by using a rotational viscometer. The probable measurement error of the viscosity was estimated to be within ± 0.5 mPa · s for the viscosity range studied here. The sample temperature was measured by using a thermistor resistance thermometer accurate to within ± 0.07°C. Figure 7 shows the measured viscosity (open circles) of the sample as a function of ΔT, and shows a least-squares approximation of the measured values (solid line). The viscosities of the sample in the supercooled state are plotted on the extrapolation curve of the least-squares approximation for the viscosity in the normal liquid phase. Figure 7 shows that the viscosity exponentially increased with degree of supercooling.

Figure 8 shows the growth rate times the sample viscosity as a function of degree of supercooling on a log scale. For $4 < \Delta T < 10$ K, the growth rate times the viscosity follows a straight line and can be expressed as a least-squares approximation:

$$v\eta_l = 9.82 \times 10^{-9}(\Delta T)^{3.25} \tag{5}$$

When $\Delta T > 10$ K, the growth rate times the viscosity disagrees with Eq. (4) as shown in Fig. 8, just as the growth rate disagrees with

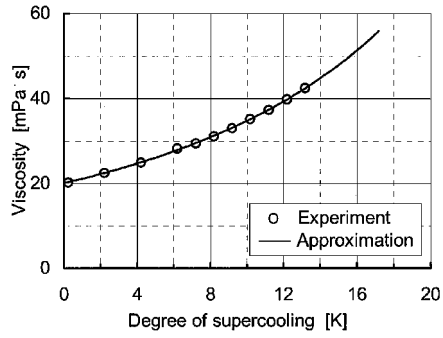

Fig. 7 Temperature dependence of viscosity of DHD.

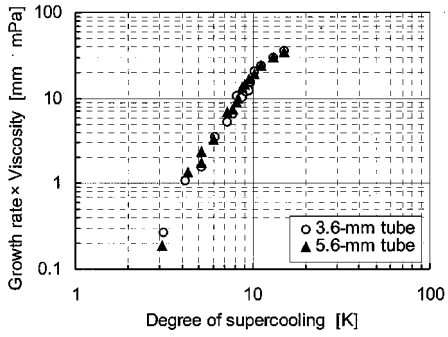

Fig. 8 Dependence of growth rate times viscosity on degree of supercooling.

Eq. (2) when $\Delta T > 10$ K. However, the disagreement between the measured values and the theoretical values with Eq. (4) is smaller than that with Eq. (2). One reason why the increment in the growth rate for high ΔT (>10–11 K) becomes small is the significant increase in viscosity with ΔT. The increase in viscosity suppresses the absorption of the molecule of the liquid sample into the crystal surface, which causes the discrepancy between actual behavior and the assumptions for Eqs. (1), (2), and (4). Another possible reason is the significant increase in the interfacial free energy between crystal and liquid. When ΔT was less than about 10–11 K, in this study the crystal of the sample grew like a single crystal. On the other hand, when ΔT was greater than about 10–11 K, the crystal grew like a dendritic crystal. Interfacial free energy depends on grain sizes and grain boundary character distributions of crystals. Because the interfacial free energy of a dendritic crystal is larger than that of a single crystal, the interfacial free energy of the DHD sample when ΔT exceeded about 10–11 K was larger than that when ΔT was less than about 10–11 K. Consequently, the increment in the growth rate with ΔT decreased as shown in Fig. 8 when the ΔT exceeded about 10–11 K.

Estimate of Critical Radius

The critical radius for homogeneous nucleation was evaluated in this study. When a cluster size in a sample reaches a critical radius r^*, the freezing rate of the sample equilibrates with the melting rate. When a cluster size exceeds r^*, nucleation occurs in the sample, and the nucleus promotes crystallization. This r^* is expressed as follows[11]:

$$r^* = \frac{2\sigma_{SL} T_e}{\Delta H \rho_s \Delta T} \tag{6}$$

The equilibrium temperature T_e is identical to the melting point under atmospheric pressure. Because measuring the interfacial free energy between the liquid and crystal is difficult, we used the following theoretical equation to evaluate the interfacial free energy[12]:

$$\sigma_{SL} = \left\{ \frac{3(\Delta H)^2 \rho_l^2 (\Delta T)^2 k T_n}{16\pi T_e^2} \ell n \left[\frac{nkT_n}{Ih} \exp\left(\frac{-\Delta F_a}{kT} \right) \right] \right\}^{\frac{1}{3}} \tag{7}$$

where T_n represents the nucleation temperature of the sample and depends on the conditions of the sample, such as volume and cooling rate. The relationship between the sample weight and ΔT was experimentally investigated. For sample weights from 0.82 to 62 mg, ΔT was measured by using DSC accurate to within ± 0.38°C. The cooling rate for DSC was 0.5 K/s. For sample weights from 0.11 to 30 g, ΔT was measured for the DHD samples in the test tubes by using thermistor resistance thermometers accurate to within ± 0.07°C. The cooling rate for the test tubes was 0.1 K/s. A previous study showed that the influence of the cooling rate of the sample on ΔT is considered negligible for a cooling rate from 0.01 to 1 K/min (Ref. 13).

Figure 9 shows the effect of sample weight on ΔT, indicating that ΔT increased as the volume of the sample decreased. The nucleation rate I is defined as the number of nuclei per second for 1 m^3 of melt. Turnbull assumed the number of nuclei generated at 1/s for a 50-μm-diam droplet of melt.[12] By extrapolation of the fitted curve in Fig. 9, the estimated ΔT of a 50-μm-diam droplet of DHD (95.7 ng) is 51.8 K. For many metals, the ratio of ΔT for a 50-μm-diam droplet to its absolute melting temperature is relatively constant, from 0.13 to 0.25, and for water, this ratio is 0.143 (Ref. 12). For the DHD sample, this ratio is 0.168, similar to that for water. For a 50-μm-diam droplet, the nucleation temperature $T_n = (T_e - \Delta T)$; for DHD, the calculated T_n is 256.9 K. The free energy of activation for transporting a molecule across a liquid–crystal interface, ΔF_a, is considered identical to the activation energy for self-diffusion.[12,14] From the measured viscosity shown in Fig. 7, ΔF_a for DHD is estimated to be 7.8×10^{-20} J/molecule. Therefore, from Eq. (7), the calculated interfacial free energy for DHD is 0.034 J/m^2.

By the use of Eq. (7), Turnbull showed that the interfacial free energy is generally 0.45 times smaller than the heat of fusion for most metals, such as iron, copper, and silver, and is 0.32 times smaller than the heat of fusion for water and a few metals, such as bismuth or germanium.[12] When it is assumed that the sample shows the same behavior as water, namely, that its interfacial energy is 0.32 times smaller than its heat of fusion, the estimated interfacial free energy is 0.092 J/m^2. One reason for the difference between the two estimates is the ideal assumptions used to derive Eq. (7), that the crystal nuclei are assumed to be spherical. Based on these two approaches to the estimation of the interfacial free energy, the interfacial free energy is estimated to be on the order of 10^{-2} J/m^2.

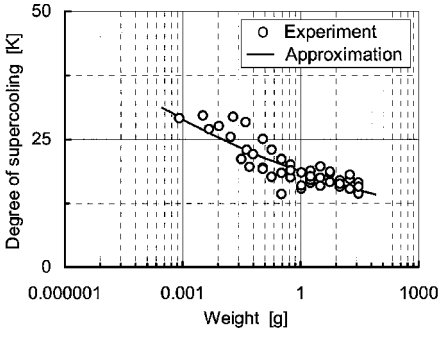

Fig. 9 Effect of sample weight on the degree of supercooling of DHD.

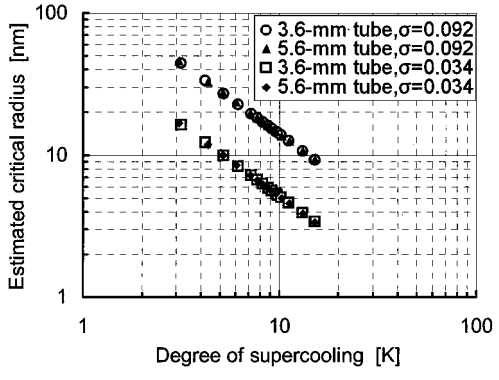

Fig. 10 Estimated critical radius for a sample of DHD.

Figure 10 shows an example of the critical radii calculated by using Eq. (6) when the interfacial energy is assumed to be 0.034 or 0.092 J/m^2 as estimated earlier. The critical radius is inversely proportional to ΔT. When $\Delta T = 10$ K, for example, the critical radius for DHD is about 100 times larger than the O–H covalent-bond length in water, 0.0957 nm, and the estimated number of the molecules in a DHD cluster of this critical radius is on the order of 10^3–10^4.

Conclusions

To develop long-term latent heat storage, Super-TES, the solidification of DHD was investigated in detail by measuring related thermophysical properties, thermal conductivity, and viscosity. The results showed that the growth rate of the DHD sample increased with increasing degree of supercooling ΔT and was slow compared with that of metals. When ΔT was less than about 10–11 K, the relationship between the growth rate and ΔT agreed with the theoretical equation that describes screw dislocation on a coarse surface. When ΔT was less than about 10–11 K, the crystal of the DHD sample grew like a single crystal, and the growth rate was approximately proportional to the third power of ΔT. Under supercooling conditions, the viscosity of the sample significantly increased as ΔT decreased, which acts to suppress the absorption of the molecule of the liquid sample into the crystal surface. When ΔT exceeded about 10–11 K, the crystal grew like a dendrite. Interfacial free energy depends on grain sizes and grain boundary character distributions of crystals, and the interfacial free energy of a dendritic crystal is larger than that of a single crystal. Because of the significant increase in viscosity and change in grain size of the crystal, the increase in the growth rate with increasing ΔT decreases when ΔT exceeds about 10–11 K. The ratio of ΔT for a small droplet (50 μm diam) of the DHD sample to its absolute melting temperature is nearly equal to that for water. The estimated interfacial free energy is on the order of 10^{-2} J/m^2. Therefore, when ΔT is 10 K, the critical radius for homogeneous nucleation of DHD is roughly 10 nm.

When DHD is used for Super-TES, nucleus formation generally starts in the lower part of the supercooled liquid because of thermal stratification, so that crystals grow upward in the storage tank. When a quick extraction of heat is required, Super-TES should be controlled while the sample is being supercooled at a temperature low enough for dendritic crystal growth because rapid growth of crystals produces a large heat-exchange area in the storage system.

Acknowledgments

We thank Kyoto Electronics Manufacturing Company, Ltd., Kyoto, Japan, and Hot Disk AB, Uppsala, Sweden, for their helpful advice in measuring the thermal conductivity of liquids by using the transient plane source technique.

References

[1]Chemical Society of Japan, "C. Determination of Purity from Melting Process," *Lecture of Experimental Chemistry 4—Heat and Pressure*, 4th ed., Maruzen, Tokyo, 1992, p. 89.

[2]Hirano, S., Saitoh, T. S., Oya, M., and Yamazaki, M., "Long-Term Supercooled Thermal Energy Storage (Thermophysical Properties of Disodium Hydrogenphosphate $12H_2O$)," *Proceedings of the 35th Intersociety Energy Conversion Engineering Conference*, Vol. 2, AIAA, Reston, VA, 2000, pp. 1013–1018.

[3]Nakae, H., "(2) Growth Rate of Dendrite," *Crystal Growth and Solidification*, Agune Syofu, Tokyo, 1998, pp. 80–83.

[4]Gustafsson, S. E., "Transient Plane Source Techniques for Thermal Conductivity and Thermal Diffusivity Measurement of Solid Materials," *Review of Scientific Instruments*, Vol. 62, No. 3, 1991, pp. 797–804.

[5]Gustavsson, M., Karawacki, E., and Gustafsson, S. E., "Thermal Conductivity, Thermal Diffusivity, and Specific Heat of Thin Samples from Transient Measurements with Hot Disk Sensors," *Review of Scientific Instruments*, Vol. 65, No. 12, 1994, pp. 3856–3859.

[6]Log, T., and Gustafsson, S. E., "Transient Plane Source (TPS) Technique for Measuring Thermal Transport Properties of Building Materials," *Fire and Materials*, Vol. 19, 1995, pp. 43–49.

[7]Hirano, S., and Saitoh, T. S., "Long-Term Supercooled Thermal Energy Storage (Thermal Conductivity of $Na_2HPO_4 \cdot 12H_2O$)," *Proceedings of the 37th National Heat Transfer Symposium of Japan*, Vol. 3, Heat Transfer Society of Japan, Tokyo, 2000, pp. 909, 910.

[8]"Thermophysical Properties of Ordinary Water," *JSME Data Book: Heat Transfer*, 4th ed., Japan Society of Mechanical Engineers, Tokyo, 1986, p. 331.

[9]Rosenberg, A., and Winegard, W. C., "The Rate of Growth of Dendrites in Supercooled Tin," *Acta Metallurgica*, Vol. 2, 1954, p. 343.

[10]Yamamoto, M., "C. Coarse Surface of Crystal," *Hand Book of Crystal Engineering*, Kyoritsu, Tokyo, 1971, pp. 151, 152.

[11]Nakae, H., "Size of Homogeneous Nuclei," *Crystal Growth and Solidification*, Agune Syofu, Tokyo, 1998, pp. 58–61.

[12]Turnbull, D., "Formation of Crystal Nuclei in Liquid Metals," *Journal of Applied Physics*, Vol. 21, No. 10, 1950, pp. 1022–1028.

[13]Hirano, S., Saitoh, T. S., Oya, M., and Yamazaki, M., "Influence of Ultrasonic Vibration on Freezing Temperature of Hydrate," *Proceedings of the 34th Intersociety Energy Conversion Engineering Conference*, Society of Automotive Engineers, Warrendale, PA, 1999. Paper 1999-01-2617.

[14]Japanese Association for Crystal Growth, "6.1.2 Steady Nucleation," *Handbook of Crystal Growth*, Kyoritsu, Tokyo, 1995, pp. 142, 143.